Compact High-Power Broadband Absorptive Filters using Slotted Waveguide Harmonic Pads

T Stander, P Meyer and PW van der Walt

Department of E&E Engineering, University of Stellenbosch
Private Bag X1, 7602 Matieland
South Africa
e-mail: pmeyer@sun.ac.za

Abstract: A compact high-power broadband absorptive filter is designed by cascading a slotted waveguide harmonic pad with a wide stop-band reflective filter. Absorption is achieved by coupling a surface current standing wave to absorptive external auxiliary waveguides through a cascade of transversal broad-wall slots in rectangular waveguide.

Keywords: absorptive filter, waveguide filter, harmonic pad, waveguide slot array, high-power filter

1. *Introduction*

Absorptive microwave filters achieve out-of-band attenuation by partial absorption rather than reflection of the signal, allowing for low input reflection coefficients at frequencies outside the pass-band. These filters find application where reflection of spurious out-of-band signals, typically generated by non-linear circuit elements, are unwanted, yet such signals must be prevented from reaching the output of the device. Typical examples include the output of mixer circuits where the reflected spurious signals can be re-introduced into the mixing process, or high-power transmitters where the reflected spurious signals can damage or de-stabilize the output amplifiers [1] .A fundamental requirement of these filters is therefore the existence of a second signal path through which only out-of-band signals are routed to internal or external absorbers (instead of being reflected back to the source), to form a frequency selective absorber.

For low-power applications, a few classes of such absorptive filters have been proposed in literature. A common approach is to load one port of a circulator or hybrid network with a frequency selective absorber which reflects energy outside of the frequency band of absorption [2, 3]. Signals within the desired filter pass-band are reflected from this network and routed to an output port via the circulator or hybrid network. Another popular class of filter is based on structures which create dual phase path cancellation [4], with approaches using digital spectrum shaping filters [5] also used. For applications requiring both a wide stop-band and high power handling capability however, the most common solution by far is the *leaky wall filter* [6, 7]. These filters attenuate an incident travelling wave in waveguide by coupling energy to an exterior structure through a series of appropriate apertures, usually narrow slots. The exterior structure may either be longitudinal auxiliary waveguides placed in parallel to the main guide [6] or individual waveguides for each aperture [7]. In both cases, the pass-band cut-off is determined by the cut-off frequency of the auxiliary waveguides, above which the energy from the main guide is coupled to the auxiliary guides and dissipated inside absorptive loads terminating the guides. This approach is highly effective, and current

high-end commercial X-band absorptive filters achieve out-of-band attenuation levels of better than 40 dB and out-of-band reflection coefficients of better than -7.5 dB over a frequency band covering three harmonics, while able to handle continuous-wave power levels of up to 500W and peak power levels of up to 5kW peak [8]. However, these filters suffer from two main drawbacks, i.e. that they are normally very bulky, and that the design process allows for very little control over the shape of the pass-band reflection response. Alternative approaches using cascades of high-power lossy resonators have been proposed [9, 10,11], but no general synthesis theory exists whereby these resonators can be utilized to design absorptive filters.

If absorption is only required in specific frequency bands in the stop-band of the filter, as is the case with the widely used harmonic filters at the outputs of transmitters, a particular approach using so-called harmonic pads [12] is of interest. A harmonic pad is effectively any device that features frequency selective absorption in a specific band and lossless transmission elsewhere. If such a device is inserted in front of a standard lossless reflective filter as shown in Fig. 1, signals in the pass-band of the reflective filter are passed with very little attenuation, while signals in the stop-band are reflected and selectively absorbed by the harmonic pad. The combined system therefore only exhibits a low input reflection coefficient in the filter pass-band and all bands in which absorption takes place, but as there is no requirement in this class of applications for low reflection outside of these bands, such a solution fulfils the system requirements. In addition, it has the significant advantage that the reflecting filter provides the stop-band attenuation for the system, while the amount of power absorbed need only be sufficient to protect the output of the source and/or prevent non-linear source behaviour due to the reflected power. Such an approach, but without implementation, has been proposed by various authors [7,13,14]. Implementations using 0 dB couplers over the signal bandwidth have been published [12], but these limit the filter transmission bandwidth to that achievable by the coupler. The use of leaky wall filters as harmonic pads has been suggested [5], but not developed in literature to date.
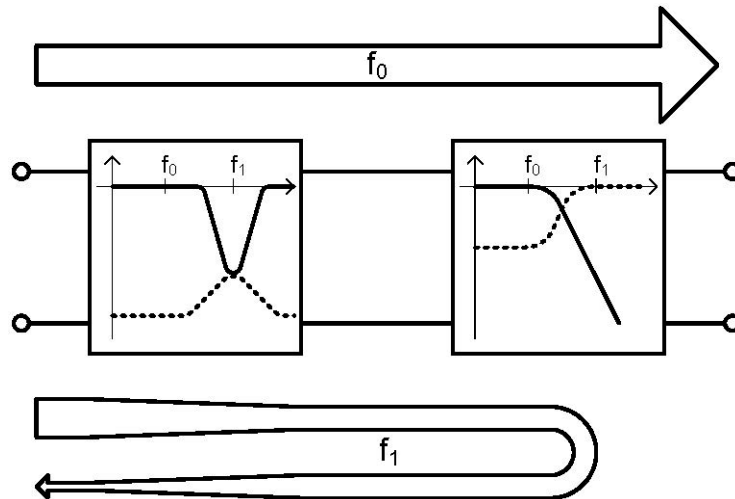

Figure 1: Block diagram of cascaded harmonic pad and reflective filter. Solid lines show S_{21} and dotted lines S_{11}

This paper develops a high-power broadband absorptive filter by cascading a novel distributed harmonic pad, consisting of a compact slotted waveguide structure, with a lossless reflective filter with a wide stop-band, both in WR-90 waveguide. A non-uniform waffle-iron filter is used as reflective filter [1], although any reflective filter can be used in principle. The slotted waveguide structure (similar to a slotted waveguide antenna, but with varying slot lengths) is designed to absorb the standing wave created by the reflective filter at a number of frequencies in the stop-band of the reflective filter, without affecting the pass-band response of the system. Using this combination, an absorptive filter is realised without the use of circulators, hybrid circuits or dual signal paths. In comparison to standard leaky-wave filters, which utilize the systematic absorption of a travelling wave to create both out-of-band attenuation and absorption of any reflected signals, the solution proposed here utilizes reflection from a standard filter to implement out-of-band attenuation, and resonant absorbers, designed to cover the frequency bands of interest, to implement partial absorption of the reflected signals. In this way, absorption levels comparable to that reported in state-of-the-art leaky-wave filters can be achieved with a structure which is significantly more compact. As example, a very compact harmonic pad is designed and tested at X-band. The pad measures only 33mm in length, yet when combined with the reflective filter, yields a reflection coefficient of below -12.5 dB in the stop band whilst attenuating the signal by better than 65dB. In all cases, circuit simulation is done using AWR Microwave Office, and full-wave simulation using CST Microwave Studio.

2. *Transversal broadwall slots in rectangular waveguide*

For use as a harmonic pad, a single waveguide slot should extract as much of the reflected energy from the main guide as possible over a specific frequency band, without affecting the pass-band transmission at other frequencies. The ideal slot should also be orientated in such a way as to reduce the overall length of the complete structure by as much as possible. To avoid excitation of higher order modes, slot arrangements that preserve both E-plane and H-plane symmetry are preferred.

A topology that satisfies all the above conditions, is the transversal broadwall slot [15], which has been shown to achieve coupling values of up to -6 dB, with a 3 dB bandwidth of 17% [16]. If a symmetric pair of centred, non-inclined slots is placed as shown in Fig. 2, both E-plane and H-plane symmetries are preserved. The width of the auxiliary guide can be reduced to increase the TE_{10} cut-off frequency of the auxiliary guide to above the main guide frequency band. This creates a natural high-pass filtering effect which inhibits energy flow to the auxiliary guide below this frequency. To absorb the power in the auxiliary guide, the broadwall of this guide is lined with an absorptive sheet of thickness $t_a = 1$ mm, and the guide is terminated at both ends with matched absorbers.
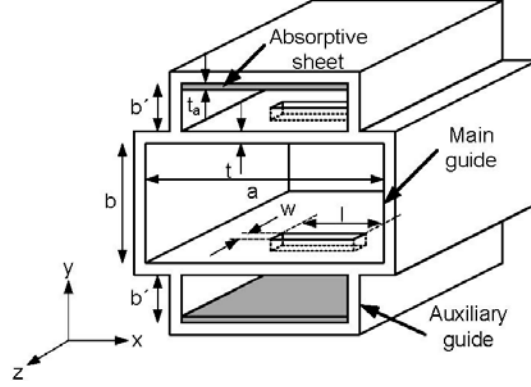
3

Figure 2: Transversal broadwall slot pair with auxiliary waveguides

The performance of such a slot pair is illustrated in Fig. 3, which shows the full-wave simulation results of a single, isolated pair of slots of length l = 8 mm and width w = 1 mm, coupling a standard X-band waveguide of wall thickness t = 1 mm to a reduced auxiliary guide of dimension 13x3mm through each broadwall, with the auxiliary guides terminated at both ends with a perfect waveguide port. Defining absorption as in equation (1),

$$A = \sqrt{1 - |S_{11}|^2 - |S_{21}|^2} \tag{1}$$

it is clear that this configuration achieves a peak absorption of -3.69 dB over a 3 dB bandwidth of 16.5% around 19.22 GHz, and a reflection coefficient of below -29 dB across the band 8.5 – 10.5 GHz. Parameter studies show that in general, the slot length l determines the frequency of maximum coupling, while the bandwidth is adjusted by varying slot width w and wall thickness t. Variation in peak absorption cannot be achieved by rotating or moving the slot from the centre axis, since this would disrupt the E-plane symmetry required to avoid the excitation of propagating even modes. However, for a fixed slot length, $|A|_{peak}$ can be adjusted by varying the auxiliary guide height b'.
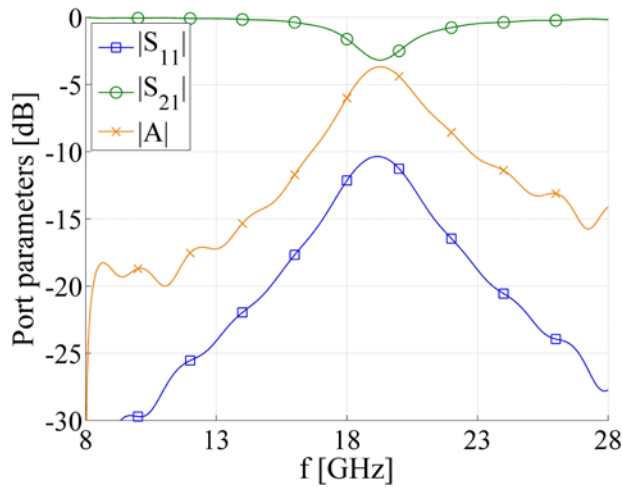

Figure 3: Transmission, reflection and absorption of transversal broadwall slot pair,
(l = 8 mm, w = 1 mm, t = 1 mm, a = 22.86 mm, b = 10.16 mm, a' = 13 mm, b' = 3 mm.)

3. *Circuit model*

Single transversal coupling slots have been studied extensively in literature, with the original classical models proposed by Oliner [17] expanded more recently using models based on full-wave electromagnetic simulations [15]. In this paper, the simple model shown in Fig. 4 is proposed for a single symmetric pair of slots such as depicted in Fig. 2. Here, the main guide is represented as a transmission line with characteristic impedance Z_0, the auxiliary guides as transmission lines of length θ_1 and characteristic impedance Z_1, terminated on both sides by a load Z_1, and the reactive coupling as a transformer and resonant circuit. To model coupling through both the floor and the roof of the main guide, one can either use two coupled circuits in series, or one coupled circuit with all the impedances doubled, as shown in Fig. 4. The latter is possible as the impedance presented to the main guide simply doubles when using slots in both broad walls.
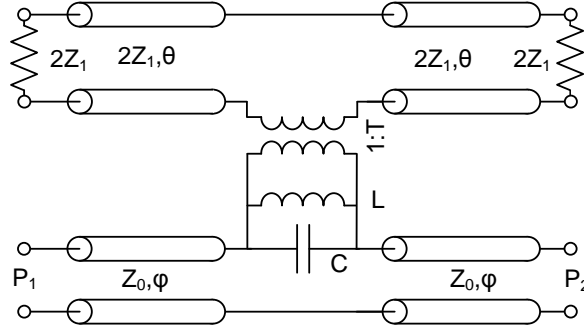

Figure 4: Circuit model of a single transversal broadwall slot pair.

This model is based on that of [15], but is reduced in complexity by the use of a single resonator, rather than two coupled resonators connected by a finite length of transmission line. In this, it is assumed that the thickness of the waveguide wall, which is modelled in [15] with a finite length transmission line, is negligible at the frequencies of interest. To determine the equivalent circuit element values, the scattering parameters of the physical structure are calculated through full-wave electromagnetic simulation, with P_2 and P_1 terminated by ideal waveguide ports. The resonator parameters are related simply by the resonant frequency

$$\omega_0 = \frac{1}{\sqrt{LC}} \tag{2}$$

at which the phase values of S_{11} and S_{21} are equal. . At this frequency, L and C cancel, and the transformer and terminated auxiliary guide can be represented by a single resistor of value R, which is related to the transformer turns ration T by

$$T = \sqrt{\frac{4Z_1}{R}} \tag{3}$$

With port P_2 of both the physical structure and the equivalent circuit terminated in a matched load, and port P_1 de-embedded to the centre of the symmetric coupling slots for both cases (i.e. by distance φ for the equivalent circuit) the input impedance at port P_1 is purely resistive at resonance. At the resonant frequency, the resistance R is then calculated from the simulated input reflection coefficient $|\Gamma| = |S_{11}|$ as

$$R = \frac{2Z_0}{1 - |\Gamma|_{\omega=\omega_0}} \frac{|\Gamma|_{\omega=\omega_0}}{} \tag{4}$$

Though it is possible to calculate L or C from the slope of the input reflection coefficient against frequency at resonance, or the wideband response of either S_{11} or S_{21}, both of these methods rely heavily on the accuracy of a few data points in a full-wave simulation, and are complicated by the presence of the embedding transmission line. A better broadband approximation is made by deriving the magnitude of the input reflection coefficient of the equivalent circuit (as referred to the de-embedded input port in the main guide) from circuit theory as

$$|\Gamma| = \frac{\omega L R}{\sqrt{\left(2RZ_0 - \frac{2\omega^2 RZ_0}{\omega_0^2}\right)^2 + (L\omega(2Z_0 + R))^2}} \tag{5}$$

The value of L (and C through equation (3)) is determined by obtaining simulated values of $|\Gamma|$ over a 25% band around the resonant frequency, and minimising the RMS error between the full-wave simulated and circuit simulated values of $|\Gamma|$. Finally, a value for φ is found by equating the transmission phase response of the full-wave simulated transmission line $\angle S_{21}$ to that of the circuit model. To illustrate this method of modelling, the full-wave S-parameters of the example structure in Fig. 2 (l=8,w=1,t=1,a=22.86,b=10.16, a'=13, b'=3) are shown in Fig. 5, together with the S-parameters of the derived model (T = 2.20, L = 400 fH, C = 173 pF, φ = 0.28°). It is evident that good agreement between full-wave and circuit models is achieved. Using two of these single-slot models separated by an ideal model of a section of TE_{10} waveguide, a combination of two of the same slots as in the previous example, cascaded with a spacing of 5 mm, is also modelled, with the results shown in Fig. 6. In both cases the frequency range is selected to represent the second harmonic of an X-band signal, and good agreement in both broadband magnitude and phase response is achieved.
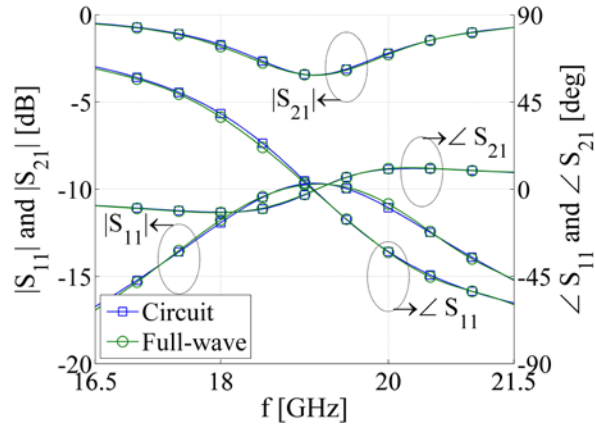
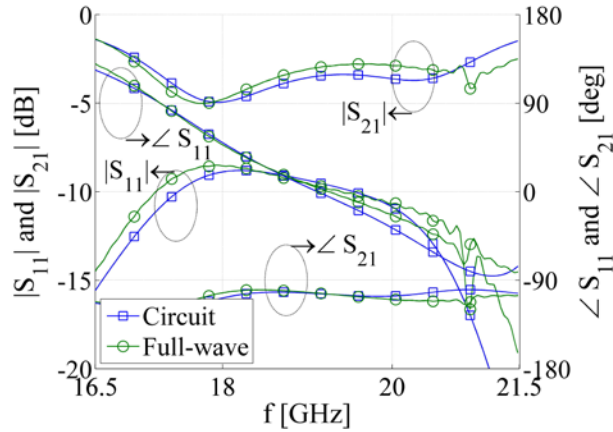Figure 5: Performance of single resonator approximation of 8 mm transversal coupling slot pair

Figure 6: Performance of cascaded coupled resonator circuit to model two slot pairs separated by 5 mm.

4. *Synthesis example*

The most applicable synthesis theories for cascaded absorptive resonators is that of Jaumann absorbers [18], which relies on analytical expressions which grow exponentially more complex for higher network orders, and is unable to accommodate arbitrary terminations. In the absence of a viable synthesis theory for the more general case, circuit model optimisation must be used to synthesise the harmonic pad. Fig.7 shows the circuit model for a triple slot structure, including circuit simulation models of perfect TE_{10} mode waveguides, cascaded with the S-parameters of a given reflective filter.
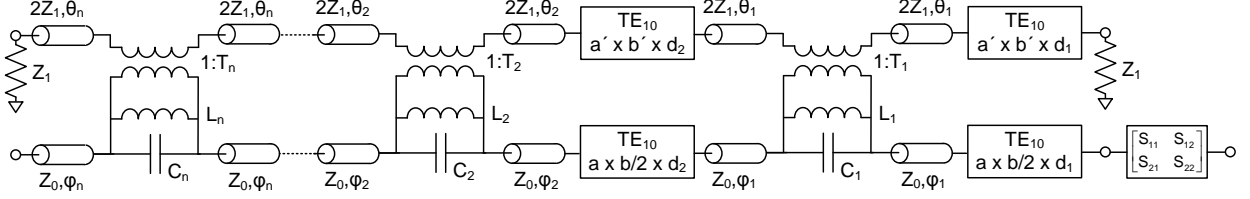
Figure 7: Triple slot circuit model cascaded with the reflective filter.

The synthesis starts by setting the initial values of the resonant frequencies f_i for all of the cascaded resonators to the centre frequency of the absorbing band, designated f_0. Initial values of a, b, a´ and b´ are based on the previously chosen values of the main and auxiliary waveguides, with initial values of L_i, C_i, φ_i and T_i derived from the previous comparison between circuit simulated and full-wave simulated responses of a single slot. This necessitates prior full-wave simulation and circuit element value definition of a single slot at the centre of the required absorbing band, as was done in Section 3. Slot spacings d_i (shown in Fig. 7) are chosen to place the slots at the standing wave pattern maxima at f_0 based on the complex input reflection of the reflective filter at f_0 and the assumption that local maxima are formed every $\lambda_{g0}/2$, where λ_{g0} is the guide wavelength at f_0. The circuit is then cascaded with the S-parameters of the given reflective filter and the values f_i and d_i are optimised to achieve a goal input reflection match over a given band using a random localised optimisation algorithm. It should be noted that each optimization update of f_i (the slot resonant frequency), and the associated update of the relevant slot length, in actual fact requires an update of all the equivalent circuit elements for that slot, which in turn requires one full-wave simulation of the updated slot. For small changes in slot length, this step can be omitted, as the other parameters are significantly less sensitive to slot length than f_i. However, any large change requires a new full-wave simulation. An alternative is to establish values of L, C, φ and T for a wide range of slot resonant frequencies (and, therefore, a wide range of slot lengths l) before circuit optimisation, and apply these changes periodically to the circuit model during optimisation using interpolation-based methods. The synthesis is considered complete when the optimisation goals are achieved with values L_i, C_i, φ_i and T_i that match the final optimised resonant frequency of each slot. The resonant frequencies are then used to find slot lengths l_i, and used in conjunction with the values of d_i to construct a full-wave model of the harmonic pad. These dimensions can then be fine-tuned in full-wave simulation to establish a final manufacturing model. Due to the accuracy of the model, in practice this tuning process results in dimensional changes of less than 10% in any of the dimensions.

As example, the procedure outlined above was applied to design a harmonic pad for an X-band (8.5-10.5 GHz pass-band) filter of which the second harmonic band (17-21GHz) is to be absorbed and not reflected. An input reflection match of -15 dB across the absorptive band was used as goal function for a five-slot structure. The full-wave simulated S-parameter data of a reflective non-uniform waffle-iron filter was used as termination of the circuit model, as shown in Fig. 7. This filter utilizes rectangular waveguide of constant width, and constant height for each section, but non-uniform boss dimensions in order to reduce size [1]. For the harmonic pad, a minimum slot spacing of $d_i > 2.4$ mm was imposed in simulation, to allow for manufacturing. The initial offset d_1 was constrained as $d_1 > 7.9$ mm, to allow for flange and an absorptive end-load to the auxiliary guide. The auxiliary guide dimensions of 13 x 3 mm were retained, as

well as the 1 mm wall thickness and 1 mm slot width. This optimisation produces the circuit values and dimensions shown in Table 1, with associated S-parameters in Fig. 10. The corresponding physical structure is shown in Fig. 8, with dimensions listed in Table 2.

Table 1: Optimised circuit parameters and associated physical dimensions.

Slot #	f [GHz]	L [fH]	C [pF]	T	φ [deg]	l [mm]	d [mm]
1	22.49	260	193	2.39	-0.45	6.75	10.81
2	18.15	487	158	2.13	-0.44	8.45	3.87
3	20.35	351	174	2.23	-0.44	7.5	2.65
4	21.00	306	188	2.30	-0.44	7.25	3.86
5	22.11	286	181	2.35	-0.44	6.87	2.58

Table 2: Initial and manufactured dimensions

Dimension	l_1	l_2	l_3	l_4	l_5	d_1	d_2	d_3	d_4	d_5
Initial [mm]	6.75	8.45	7.5	7.25	6.87	10.8	3.87	2.65	3.86	2.58
Tuned [mm]	6.42	8.45	7.5	7.23	6.87	10.2	3.75	2.42	3.60	2.65
Variation [%]	-4.89	0	0	-0.28	0	-5.64	-3.10	-8.68	-6.74	+2.71

The final dimensions were obtained after a short additional full-wave optimisation stage aimed at reducing the reflection in the absorption band, during which no dimension had to be tuned by more than 10% of its initial value. The full-wave analysis of the final structure is shown in Figures 9 and 10. It is clear that the technique produces an absorptive filter with good matching in both pass-band and absorptive band.
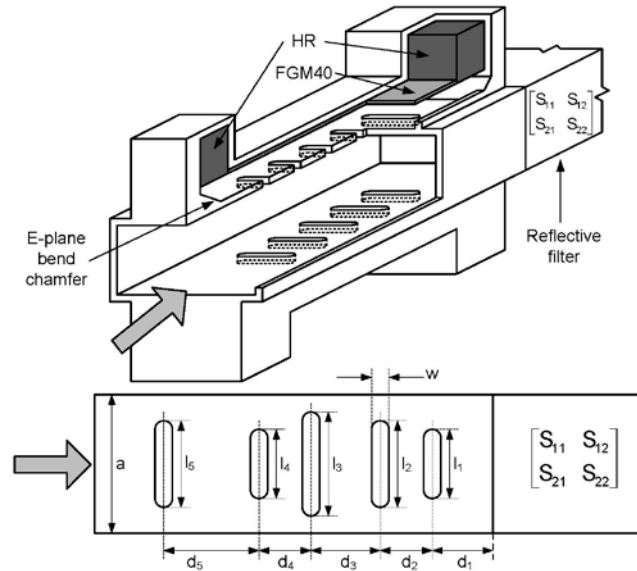

Figure 8: Final harmonic pad. Note the two end-loads to the auxiliary guide
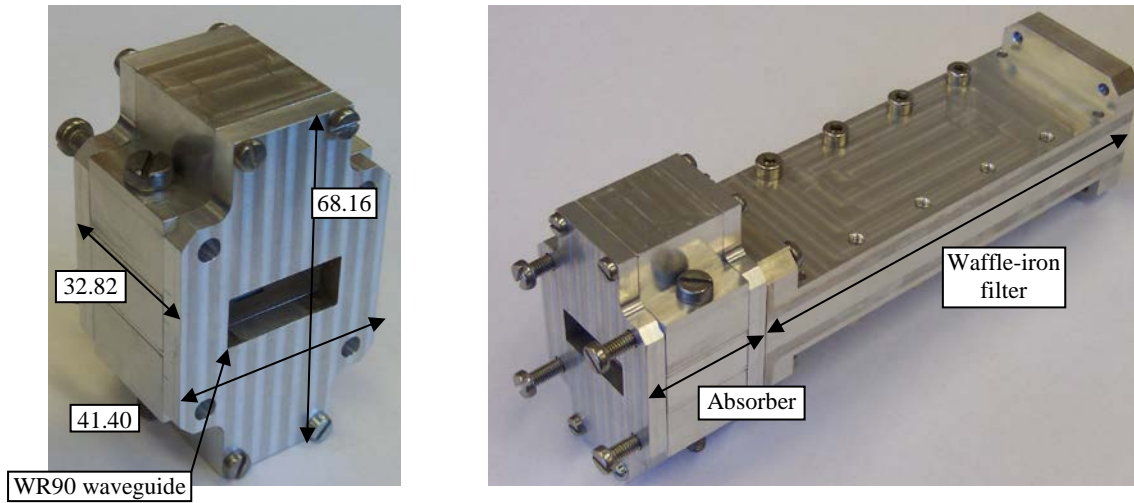made from Eccosorb™ HR and placed in E-plane bends.

9

Figure 9: Manufactured harmonic pad (left) and applied to a reflective waffle-iron filter [1] (right).
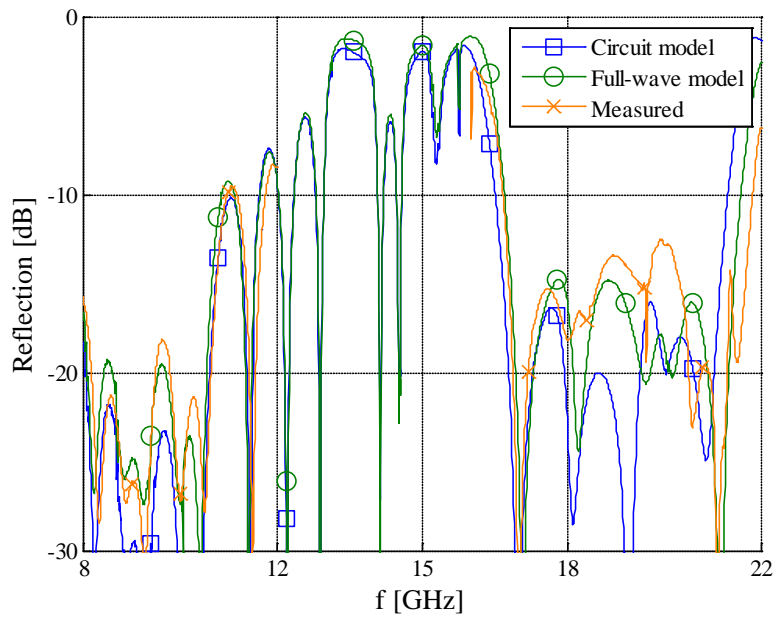

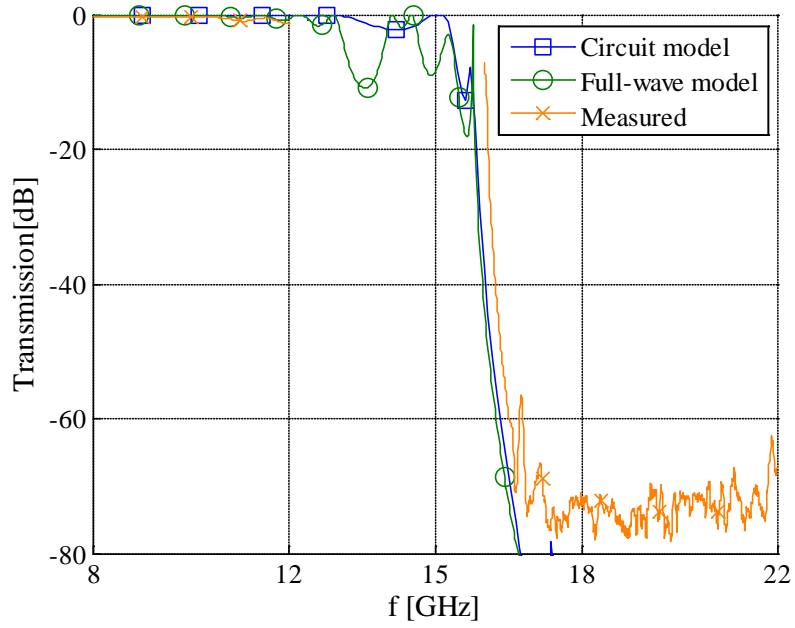Figure 10: Measured and simulated reflection response.

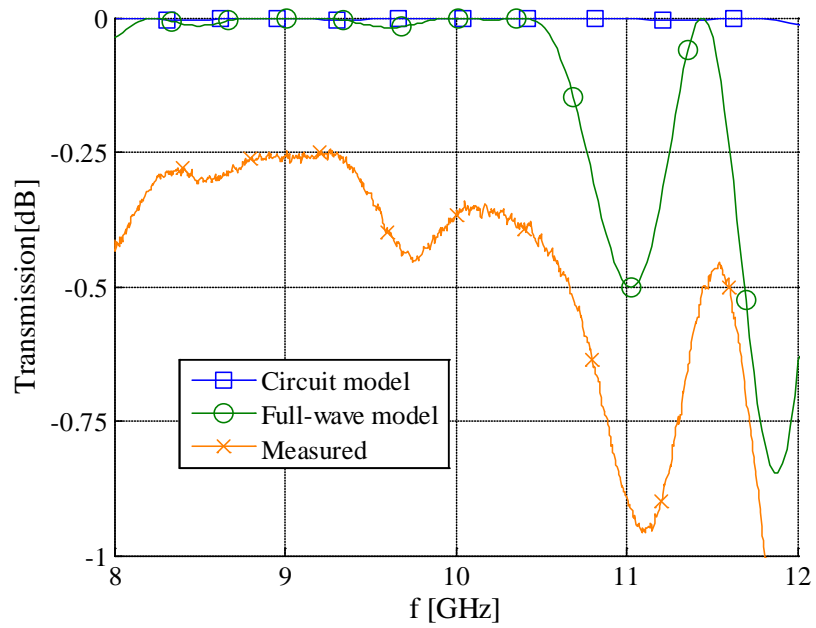Figure 11: Measured and simulated transmission response, wideband.

Figure 12: Measured and simulated transmission response, narrowband.

5. *Peak power handling capability*

The peak power handling capability of the structure is determined by finding the maximum E-field strength E_{max}, and comparing it to the breakdown E-field strength E_B. From simulation, the maximum E-field occurs at resonance across the slot aperture. At 19 GHz, the simulation indicates E_{max} = 36996 V/m RMS for 1W RMS incident power, which translates to a peak incident power P_{max} 1.086 kW if value of E_{max} = 12.1 kV/cm RMS is chosen to avoid sparking across the aperture of the slot. Away from slot resonance, the slot exhibits maximum power handling capabilities comparable to the waveguide itself, since there is no concentration of E-field in or around the slot.

6. *Manufacturing and measured results*

The harmonic pad was manufactured from Aluminium 6082 (Fig. 9), using Eccosorb[TM] FGM-40 as sheet absorber lining the opposing broadwall in the auxiliary guide. The absorptive end-loads in the auxiliary guides were implemented with Eccosorb[TM] HR in an E-plane bend, to make the load (and, consequently, the pad itself) more compact. The harmonic pad has a total length of 33 mm, flanges included. The harmonic pad was attached to an existing non-uniform waffle-iron filter, with the total measured S-parameters shown in Figs. 10, 11 and 12. Calibration was performed over the bands 8 – 12 GHz and 16 – 22 GHz, to cover the transmission and absorption bands of interest. A full two-port coaxial calibration at the coaxial-waveguide transitions was completed, followed by a TRL waveguide calibration for respectively the two bands of interest. For the TRL calibrations, the Line-standards were implemented using short sections of WR90 waveguide between the transitions. The complete absorptive filter exhibits -18 dB input reflection across the 8.5-10.5GHz pass-band (Fig. 10), and -12.5 dB peak reflection in the absorptive band. The combined structure exhibits insertion loss of more than 65dB in the absorptive band (Fig. 11) but less than 0.5dB in the pass-band (Fig. 12). The discrepancies in simulated and measured response are attributed to some discrepancy between the full-wave simulated S-parameter data of the reflective filter (used to design the harmonic pad) and the manufactured S-parameter measurement data of the the waffle-iron filter. Nevertheless, the results indicate good agreement between synthesised and measured responses.

7. *Conclusion*

This paper presents an approach for the development of compact harmonic pads using transversal broadwall slots in rectangular waveguide coupling to absorptive auxiliary guides. Good first-iteration synthesis accuracy is achieved in a band 17 - 21 GHz, producing matching over a 20% bandwidth to below -12.5 dB.

8. *Acknowledgements*

9.   *References*

1. T. Stander, High-power broadband absorptive waveguide filters, PhD dissertation, University of Stellenbosch, 2009. Available online http://scholar.sun.ac.za/handle/10019.1/1157

2. J. D. Rhodes, Microwave reflection filter including a ladder network of resonators having progressively smaller Q values, U.S. Patent 5 781 084, July 14, 1998.

3. E. N. Torgow, Hybrid junction-cutoff waveguide filters, IRE Trans Microwave Theory and Tech 7 (1959), 163–167.

4. D. R. Jachowski, Passive enhancement of resonator Q in microwave notch filters, IEEE MTT-S International Microwave Symposium Digest 3 (2004), 1315–1318.

5. A. R. Djordjevic and A. G. Zajic, Low-reflection bandpass filters with a flat group delay, IEEE Trans Microwave Theory and Tech 53 (2005) 1164–1167.

6. S. Conning, High-power harmonic suppression filters, U.S. Patent 3 496 497, February 17, 1970.

7. V. O. Met, Absorptive filters for microwave harmonic power, Proc IRE 47 (1959), 1762–1769.

8. ME Corporation, Waveguide harmonic absorption filters, Data Sheet T41C (2005).

9. L. B. Minakova and L. A. Rud, Resonance absorption in single and cascaded lossy waveguide-dielectric resonators, Microwave Opt Tech Letters 36 (2003), 122–126.

10. L. B. Minakova and L.A. Rud, Natural-Frequency Approach to the Synthesis of Narrow-Band Waveguide Absorption Filters, Proceedings of the 32nd European Microwave Conference 1 (2002), 1–4.

11. S. G. Tantawi and A. E. Vlieks, Compact X-band high power load using magnetic stainless steel, Proceedings of the 1995 Particle Accelerator Conference 4 (1995), 2132–2134.

12. L. Young, Waveguide 0-db and 3-db directional couplers as harmonic pads, Microwave Journal 7 (1964), 79–87.

13. L. Young, B. M. Schiffman and E. G. Cristal, High-power filters for the suppression of spurious frequencies, PTGMTT International Symposium Digest 64 (1964)

14. L. Young, The design of branch-guide couplers, with applications to the suppression of spurious frequencies, PGMTT National Symposium Digest 62 (1962)

15. I. A. Eshrah, A. A. Kishk, A. B. Yakovlev, and A. W. Glisson, Generalized equivalent circuit model for transverse waveguide slots and applications, Progress in Electromagnetics 69 (2007), 1–20.

16. A. Datta, A. M. Rajeek, A. Chakrabarty, and B. N. Das, S-matrix of a broad wall coupler between dissimilar rectangular waveguides, IEEE Trans Circuit Theory 43 (1995), 56–62.

17. A. A. Oliner, The impedance properties of narrow radiating slots in the broad face of rectangular waveguide: Part II, IRE Trans Antennas Propagat 5 (1957), 4–11.

18. L. J. du Toit, Advances in the design of Jaumann absorbers, Proc. IEEE APS Int. Symp, vol. 3 (1990).